STEM CELLS AND DEVELOPMENT
Volume 22, Number 8, 2013

DOI: 10.1089/scd.2012.0244

Enrichment and Characterization of Human Dermal Stem/Progenitor Cells by Intracellular Granularity

Joong Hyun Shim, Tae Ryong Lee, and Dong Wook Shin

Adult stem cells from the dermis would be an attractive cell source for therapeutic purposes as well as studying the process of skin aging. Several studies have reported that human dermal stem/progenitor cells (hDSPCs) with multipotent properties exist within the dermis of adult human skin. However, these cells have not been well characterized, because methods for their isolation or enrichment have not yet been optimized. In the present study, we enriched high side scatter (SSC^{high})-hDSPCs from normal human dermal fibroblasts using a structural characteristic, intracellular granularity, as a sorting parameter. The SSC^{high}-hDSPCs had high in vitro proliferation properties and expressed high levels of *SOX2* and *S100B*, similar to previously identified mouse $SOX2^+$ hair follicle dermal stem cells. The SSC^{high}-hDSPCs could differentiate into not only mesodermal cell types, for example, adipocytes, chondrocytes, and osteoblasts, but also neuroectodermal cell types, such as neural cells. In addition, the SSC^{high}-hDSPCs exhibited no significant differences in the expression of nestin, vimentin, *SNAI2*, *TWIST1*, versican, and *CORIN* compared with non-hDSPCs. These cells are therefore different from the previously identified multipotent fibroblasts and skin-derived progenitors. In this study, we suggest that hDSPCs can be enriched by using characteristic of their high intracellular granularity, and these SSC^{high}-hDSPCs exhibit high in vitro proliferation and differentiation potentials.

Introduction

Adult stem cells have attracted much attention because of their possible use as a cell replacement therapy, as a key tool for understanding how humans develop, as a means of screening drugs, and as delivery vehicles for molecular medicine [1]. These adult stem cells have the self-renewal ability and can differentiate into cell types present in other organs, either in vitro or in vivo [2–10]. Adult stem cells exist in multiple tissues of the body, including the bone marrow [2–5], brain, skeletal muscle [6], adipose tissue [7,8], umbilical cord [9], and placenta [10]. The skin is the largest organ in the body, and its stem cells have been identified in all regions of the skin, including the epidermis [11,12], dermis [13–20], and hair follicles [21,22].

Although many scientists have tried to identify universal dermal stem cell markers, no specific markers have been accepted. SOX2 is an SRY-related transcription factor that promotes somatic stemness, and that is expressed in the dermal papilla [23,24]. SOX2 is known to play an essential role in maintaining self-renewal of embryonic stem cells and is 1 of the 4 reprogramming factors (SOX2, OCT-3/4, KLF4, and c-Myc) used to dedifferentiate somatic cells into the induced pluripotent stem cells [25,26]. SOX2 was recently reported to be expressed in adult stem cells, where it may have a specific function in their differentiation and growth [27]. Biernaskie et al. [18] sorted skin-derived progenitors (SKPs) from the mouse using a vector carrying enhanced green fluorescent protein (EGFP) under the control of the *SOX2* gene promoter (*SOX2*:EGFP). They demonstrated that multipotent SKPs derived from $Sox2^+$ cells display dermal stem cell properties, including wound healing, hair follicle regeneration, and dermal homeostasis.

If human dermal stem/progenitor cells (hDSPCs) could be easily isolated from human dermal fibroblasts, they would become a useful resource for stem cell-based therapies as well as a good tool for researching the homeostatic and regenerative capacity of many human tissues and organs. At present, no specific cell surface markers are available for distinguishing hDSPCs in culture systems. The development of a method to enrich these cells is therefore a prerequisite for their future application. We previously demonstrated that collagen type IV-sorted hDSPCs (cells adhered within 5 min on the collagen type-IV-coated culture dishes) showed stem cell-like characteristics [28]. Compared with collagen type IV-sorted non-hDSPCs (cells adhered between 5 min and 12 h on the collagen type IV-coated culture dishes), collagen type IV-sorted hDSPCs can form many colonies, in vitro proliferate relatively rapidly, and differentiate into mesodermal progenies, including adipocytes, chondrocytes, and osteoblasts, and neuroectodermal progeny such as neural cells.

Bioscience Research Institute, Amorepacific Corporation R&D Center, Yongin-si, Republic of Korea.

In this study, we found that collagen type IV-sorted hDSPCs had higher intracellular granularity than collagen type IV-sorted non-hDSPCs by flow cytometry. Therefore, we isolated the cells with high intracellular granularity (high side scatter [SSC^{high}]) from normal human dermal fibroblasts (NHDFs). These cells, termed SSC^{high}-hDSPCs, expressed 2 specific markers, *SOX2* and *S100B*. The SSC^{high}-hDSPCs were differentiated into adipogenic, osteogenic, chondrogenic, and neurogenic cells under defined conditions.

Materials and Methods

Cell culture

NHDFs (Lonza) are derived from the breast or abdomen (man, 18 years, Black; woman, 38 years, Black; woman, 41 years, Asian) or neonatal foreskin (each $n=3$).

NHDFs were cultured in the Dulbecco's modified Eagle's medium (DMEM; Lonza) containing 10% fetal bovine serum (FBS; Lonza), 100 U/mL penicillin, and 100 μg/mL streptomycin at 37°C in 5% CO_2. NHDFs were used for the experiments within 3 passages.

Fluorescence-activated cell sorter analysis of collagen type IV-sorted hDSPCs

Collagen type IV (Sigma)-coated dishes were prepared by coating 100-mm dishes with collagen type IV (20 μg/mL) overnight at 4°C. NHDFs were plated onto collagen type IV-coated dishes and were then sorted on the basis of their ability to adhere to collagen type IV within 5 min (collagen type IV-sorted hDSPCs) or within 12 h (non-hDSPCs) at 37°C as described previously [28]. Each collagen type IV-sorted hDSPCs and collagen type IV-sorted non-hDSPCs was washed with phosphate-buffered saline (PBS) 3 times, and cell suspensions were filtered through BD Falcon Cell-Strainer Caps. Each specific region of collagen type IV-sorted hDSPCs and collagen type IV-sorted non-hDSPCs was sorted as R1, R2, and R3, respectively, for flow cytometric analysis with a fluorescence-activated cell sorter (FACS), FACSCalibur (BD Biosciences), which measured forward scatter (FSC; a relative measure of cell size) and SSC (a relative measure of intracellular granularity).

Enrichment of hDSPCs using high intracellular granularity (SSC^{high}-hDSPCs)

To isolate SSC^{high}-hDSPCs, NHDFs were resuspended in PBS containing 1 μg/mL of 4′,6-diamidino-2-phenylindole dihydrochloride (DAPI; Sigma) and filtered through a 100-μm nylon mesh. FACSAria II (BD Biosciences) was used for sorting and analysis. On the basis of FACS analysis by collagen type IV-mediated enrichments (Fig. 1), the gate of SSC^{high} was determined as top 3.5% cells in SSC. The set point of FSC^{high}/FSC^{low} was selected as previously

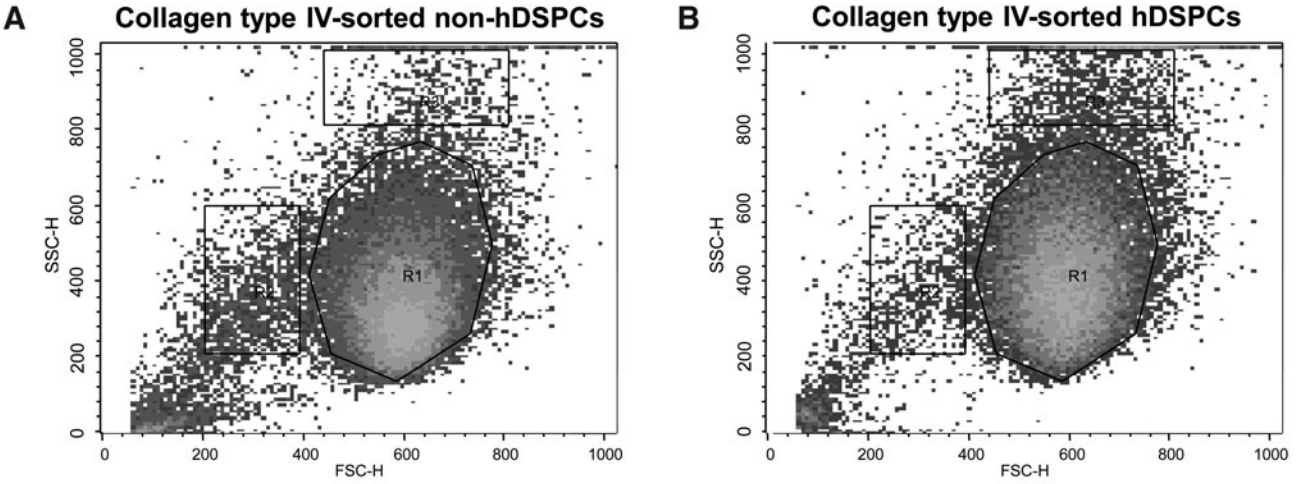

C

		R1	R2	R3
Percentage (%) of total cells	Collagen type IV-sorted non-hDSPCs	82.05 ± 2.7	3.87 ± 0.12	1.1 ± 0.05
	Collagen type IV-sorted hDSPCs	80.45 ± 3.6	2.38 ± 0.15	3.3 ± 0.1

FIG. 1. Flow cytometry analysis of collagen type IV-sorted hDSPCs and non-hDSPCs. **(A, B)** The SSC^{high} fraction of the collagen type IV-sorted hDSPCs group was increased 3-fold as compared with the collagen type IV-sorted non-hDSPCs group. A representative sample is shown for each condition ($n=3$). **(C)** Relative distributions of specific structural properties in 2 groups of cells isolated from NHDFs using collagen type IV. hDSPCs, human dermal stem/progenitor cells; FSC, forward scatter; SSC, side scatter; NHDFs. normal human dermal fibroblasts.

described [3]. Thus, sorting parameters were set as follows. Each specific region of NHDFs was gated as the Q1, Q2, Q3, and Q4 region (Q1: $FSC^{low}SSC^{high}$; Q2: $FSC^{high}SSC^{high}$; Q3: $FSC^{low}SSC^{low}$; Q4: $FSC^{high}SSC^{low}$), respectively. Nozzle diameter was set at 70 μm, and flow velocity was determined as follows: FSC^{low}/SSC^{high}, 23; FSC^{high}/SSC^{high}, 271; FSC^{low}/SSC^{low}, 1,427; FSC^{high}/SSC^{low}, 5,932.

Colony-forming assay

SSC^{high}-hDSPCs were isolated from NHDFs by an FACS analysis. Before cell seeding, a 6-well plate was coated with 0.1% gelatin (Sigma) for 30 min at 37°C. About 5×10^2 cells were seeded in a gelatin-coated 6-well plate and grown at 37°C in 10% FBS-DMEM. Cells were grown for 10 days and then photographed using a digital camera system (Canon). Growth capacity was visualized on day 10 by staining cultured cells with 0.1% crystal violet in 10% ethanol for 5 min at room temperature (RT) and then rinsing with PBS 4 times.

In vitro cell proliferation assay

After sorting, the proliferation capacity was measured with the cell counting kit-8 (CCK-8 kit; Dojindo). Cells were treated with 100 μL of the CCK-8 solution in 1 mL of DMEM, incubated for 1 h at 37°C, and the optical density was measured at 450 nm with a SpectraMax 190 microplate reader (Molecular Devices).

RNA isolation and real-time reverse transcription–polymerase chain reaction

Total RNA was extracted using Trizol™ (Invitrogen), and RNA concentrations were determined using a NanoDrop spectrophotometer (Thermo Scientific). Four micrograms of RNA was reverse-transcribed into cDNA using SuperScript® III reverse transcriptase (Invitrogen). The reverse transcription reaction was stopped by adding the Tris–ethylenediaminetetraacetic acid buffer (pH 7.8) to a total of 200 μL of cDNA solution. Real-time reverse transcription–polymerase chain reaction (RT-PCR) was performed according to the manufacturer's instructions. Briefly, the 20-μL PCR reaction contained 10 μL of 2×TaqMan® universal II PCR Master Mix, 1 μL of 20×TaqMan Gene Expression assay with FAM™ dye-labeled TaqMan MGB probe (Applied Biosystems), and 50 ng of cDNA. Real-time RT-PCR was performed with a 7500 Fast Real-Time PCR System (Applied Biosystems). cDNA samples were analyzed for the following genes: *SOX2* (Hs01053049_s1); *S100B* (Hs00389217_m1); nestin (Hs00707120_s1); vimentin (Hs00185584_m1); osteoglycin (Hs00247901_m1); osteocalcin (Hs01587814_g1); peroxisome proliferator-activated receptor-gamma (*PPARγ*; Hs01115513_m1); leptin (Hs00174877_m1); adiponectin (Hs00605917_m1); fatty acid-binding protein 4 (*FABP4*; Hs00609791_m1); aggrecan (Hs00153936_m1); collagen type 2 alpha (*COL2A1*; Hs00264051_m1); microtubule-associated protein 2 (*MAP2*; Hs00258900_m1); *SNAI2* (Hs00950344_m1); *TWIST1* (Hs00361186_m1); versican (Hs00171642_m1); *CORIN* (Hs00198141_m1); human *GAPDH* (43333764F) (Applied Biosystems). Gene expression data were analyzed as per the manufacturer's instruction. The baseline and threshold values were set to determine the threshold cycles (C_T) for the amplification curves. Then, relative expression of each gene was calculated by using the comparative C_T method. *GAPDH* was used as normalization control.

In vitro differentiation

Isolated SSC^{high}-hDSPCs were analyzed for their capacity to differentiate into adipogenic, osteogenic, chondrogenic, and neural lineages. The differentiation medium was changed every 2–3 days.

Adipogenic differentiation was induced in an adipogenic medium (1 g/L glucose-DMEM supplemented with 10% FBS, 100 U/mL penicillin, 100 μg/mL streptomycin, 0.5 mM 3-isobutyl-1-methylxanthine (IBMX), 1 μM dexamethasone, 10 μg/mL insulin, and 2 μM troglitazone (Sigma) for 2 weeks [29].

To induce osteogenic differentiation, the cells were treated with the human mesenchymal stem cell (hMSC) Osteogenic BulletKit (Lonza) for 3 weeks [30].

For chondrogenic differentiation, cells were cultured with the hMSC Chondrogenic Bulletkit (Lonza) for 2 weeks [31].

To induce neural differentiation, the cells were plated on culture plates coated with laminin (0.02 mg/mL; Sigma) and poly-D-lysine (0.2 mg/mL; Sigma) [18]. Cells were maintained in the DMEM supplemented with 10% FBS, 100 U/mL penicillin, and 100 μg/mL streptomycin for 24 h. Neural differentiation was induced by exposing cells to 10 ng/mL basic fibroblast growth factor (bFGF) (R&D Systems) for 24 h, followed by 2 days of treatment with 1 mM β-mercaptoethanol (Invitrogen) and 10 ng/mL NT-3 (R&D Systems). Finally, cells were treated with 10 ng/mL NT-3, 10 ng/mL nerve growth factor (NGF) and 50 ng/mL brain-derived neutrophic factor (BDNF) (R&D Systems) in the DMEM for 7 days [32].

Histochemical analyses

The presence of intracellular lipid droplets in differentiated adipocytes was verified by Oil-Red-O staining. Cells were fixed for 10 min at RT in 4% paraformaldehyde and then washed with 60% isopropanol. The cells were then incubated in an Oil-Red-O staining solution (Sigma) at RT for 10 min. Excess stain was removed by washing with 70% ethanol, followed by a wash with double-distilled water. The Oil-Red-O contents were then extracted with 100% isopropanol and quantified with a SpectraMax 190 microplate reader at 500 nm.

The chondrogenic differentiation was detected by Safranin-O staining. Cells were fixed with 4% paraformaldehyde for 10 min, washed with double-distilled water, and stained with 0.6% Safranin O in 20% ethanol (Sigma) for 2 min.

To examine osteogenic differentiation, an alkaline phosphatase (ALP) staining kit (Takara) was used. Briefly, cells were fixed with a citrate buffer (pH 5.4) containing 10% methanol and 45% acetone for 5 min at RT. The cells were then incubated in an ALP substrate for 30 min at 37°C and washed 3 times with double-distilled water.

Immunofluorescence

Cells were fixed with 4% paraformaldehyde at RT for 10 min and then permeabilized with 0.3% Triton X-100 with PBS with 0.05% Tween 20 (PBST) for 15 min. Blocking and diluent solutions contained PBST and 10% normal goat

serum (Jackson ImmunoResearch). Cells were blocked at RT for 30 min, incubated for 1.5 h with primary antibodies against Ki67 (ab15580-100; Abcam; 1:1,000), perilipin (ST1592; Calbiochem; 1:500), osteocalcin (ab13420; Abcam; 1:500), Sox9 (ab26414; Abcam; 1:500), beta III tubulin (Tuj1) (ab7751; Abcam; 1:1,000), and MAP2 (5H11; Novus; 1:1,000), and then incubated with Alexa-488- or 594-conjugated secondary antibodies (Invitrogen) for 1.5 h at RT. The nuclei were stained with 5 μg/mL of DAPI (Sigma) for 5 min. PBST was used for the washes between each step. Slide-mounted samples were imaged with an EVOS fluorescence microscope (Advanced Microscopy Group).

Statistical analysis

Data were analyzed by one-way analysis of variance or Student's *t*-test with MINITAB software (Minitab, Inc.), and were presented as the mean ± standard deviation of at least 3 independent experiments. The threshold of significance was set at $P < 0.05$.

Results

Characterization of hDSPCs enriched with collagen type IV

We previously demonstrated that hDSPCs can be enriched using collagen type IV [28]. Briefly, when NHDFs were plated onto collagen type IV-coated culture dishes, a portion of the population adhered to the culture dish. Cells adhering within 5 min (collagen type IV-sorted hDSPCs) or between 5 min and 12 h (collagen type IV-sorted non-hDSPCs) were separated and transferred to different culture dishes.

To characterize these 2 cell populations, the collagen type IV-sorted hDSPCs and collagen type IV-sorted non-hDSPCs were analyzed by flow cytometry. These hDSPCs and non-hDSPCs are plotted according to the cell size (FSC) and intracellular granularity (SSC) (Fig. 1). Each population was defined into 3 regions by their light-scattering characteristics. Interestingly, we found that the cell number in the R3 region of collagen type IV-sorted hDSPCs was increased ~3-fold compared with collagen type IV-sorted non-hDSPCs ($P < 0.01$). In contrast, the cell number in the R2 region in collagen type IV-sorted hDSPCs was decreased by about 40% compared with collagen, type IV-sorted non-hDSPCs ($P < 0.01$) (Fig. 1C).

SSC^{high}-hDSPCs possess high in vitro proliferative potential and express putative dermal stem cell markers

Next, NHDFs were subfractionated, and 4 subpopulations were defined as follows. That is, based on the FACS analysis of collagen type IV-sorted hDSPCs (Fig. 1), SSC^{high} was selected as top 3.5% cells in SSC. The criteria of FSC^{high}/FSC^{low} for experimental analysis were determined according to previous report, which suggests that MSCs are generally <0.2% of whole cells inside tissues [3,33,34] (Fig. 2A; Supplementary Fig. S1; Supplementary Data are available online at www.liebertpub.com/scd; Q1: $FSC^{low}SSC^{high}$; Q2: $FSC^{high}SSC^{high}$; Q3: $FSC^{low}SSC^{low}$; Q4: $FSC^{high}SSC^{low}$).

According to several previous reports [18,19], $SOX2^+$ dermal precursors and SKPs share similar function and transcriptional profile. To assess that subfractionated cells in Q1 or Q2 (SSC^{high}) may have similarity with $SOX2^+$ dermal precursors and SKPs at a molecular level. Real-time RT-PCR analysis was performed. The results revealed that cells in Q1 or Q2 (SSC^{high}) express high levels of *SOX2* and *S100B* mRNA compared with cells in Q3 or Q4 (SSC^{low}) ($P < 0.01$) (Fig. 2B). Therefore, we fractionated NHDFs into 2 subpopulations with SSC^{high} (SSC^{high}-hDSPCs) and SSC^{low} (non-hDSPCs) by using high-intracellular-granularity criteria (<3.5% cells of total NHDFs), regardless of the FSC value. Phase-contrast images showed that isolated SSC^{high}-hDSPCs have higher intracellular granularity than non-hDSPCs, in accordance with the FACS analysis (Fig. 2C).

Recent studies demonstrated that multipotent fibroblasts clonally isolated from human dermis are negative for nestin and positive for vimentin [16]. Another group reported that SKPs express both nestin and vimentin [13,15]. Thus, the characteristics of SSC^{high}-hDSPCs at a molecular level were examined by real-time RT-PCR analysis. Interestingly, we found that there were no significant differences in the mRNA expression levels of nestin and vimentin between the SSC^{high}-hDSPCs and non-hDSPCs ($P > 0.05$) (Supplementary Fig. S2A, B). In addition, real-time RT-PCR analysis revealed that there were no significant differences in the expression levels of SKP markers, such as *SNAI2* and *TWIST1*, and dermal papilla markers such as versican, *CORIN* between 2 cell populations ($P > 0.05$) (Supplementary Fig. S2C–F).

Colony-forming assay provides a convenient method of measuring the proliferative capacity that MSCs retain [35–37]. To examine growth capacity, isolated cells from each cell population were seeded on gelatin-coated 6-well culture plates in triplicate at a density of 5×10^2 cells per well. Compared with non-hDSPCs, SSC^{high}-hDSPCs produced a large number of colonies after 10 days of culture (Fig. 2D). CCK-8 analysis also showed that SSC^{high}-hDSPCs were significantly more proliferative than non-hDSPCs ($P < 0.01$) (Fig. 2E). In addition, we found that the number of SSC^{high}-hDSPCs stained with proliferation marker Ki67 antibody was larger than that of non-hDSPCs ($P < 0.01$) (Fig. 2F). These results indicate that these SSC^{high}-hDSPCs have high in vitro proliferative potential compared with non-hDSPCs.

According to previous reports [13,15,38], we further examined whether SSC^{high}-hDSPCs can be able to form floating spheres in the SKP medium, which is supplemented with both bFGF and epidermal growth factor (EGF). We found that SSC^{high}-hDSPCs showed higher gene expression level of both *SOX2* and *S100B* under the SKP medium than the 10% FBS-DMEM ($P < 0.01$) (Supplementary Fig. S3B), suggesting that the SKP medium is more suitable for maintaining the characteristics of SSC^{high}-hDSPCs than the 10% FBS-DMEM.

Analysis of SSC^{high}-hDSPC multipotency

The multipotency of SSC^{high}-hDSPCs was evaluated by inducing the cells to differentiate into mesodermal cell types (adipogenic, osteogenic, and chondrogenic) and neural lineages under specific culture conditions, as described in the section Materials and Methods.

Adipogenic differentiation was ascertained by Oil-Red-O staining. Oil-Red-O accumulation demonstrated that SSC^{high}-hDSPCs can more efficiently differentiate into an adipogenic lineage than non-hDSPCs (Fig. 3A). About 35% of

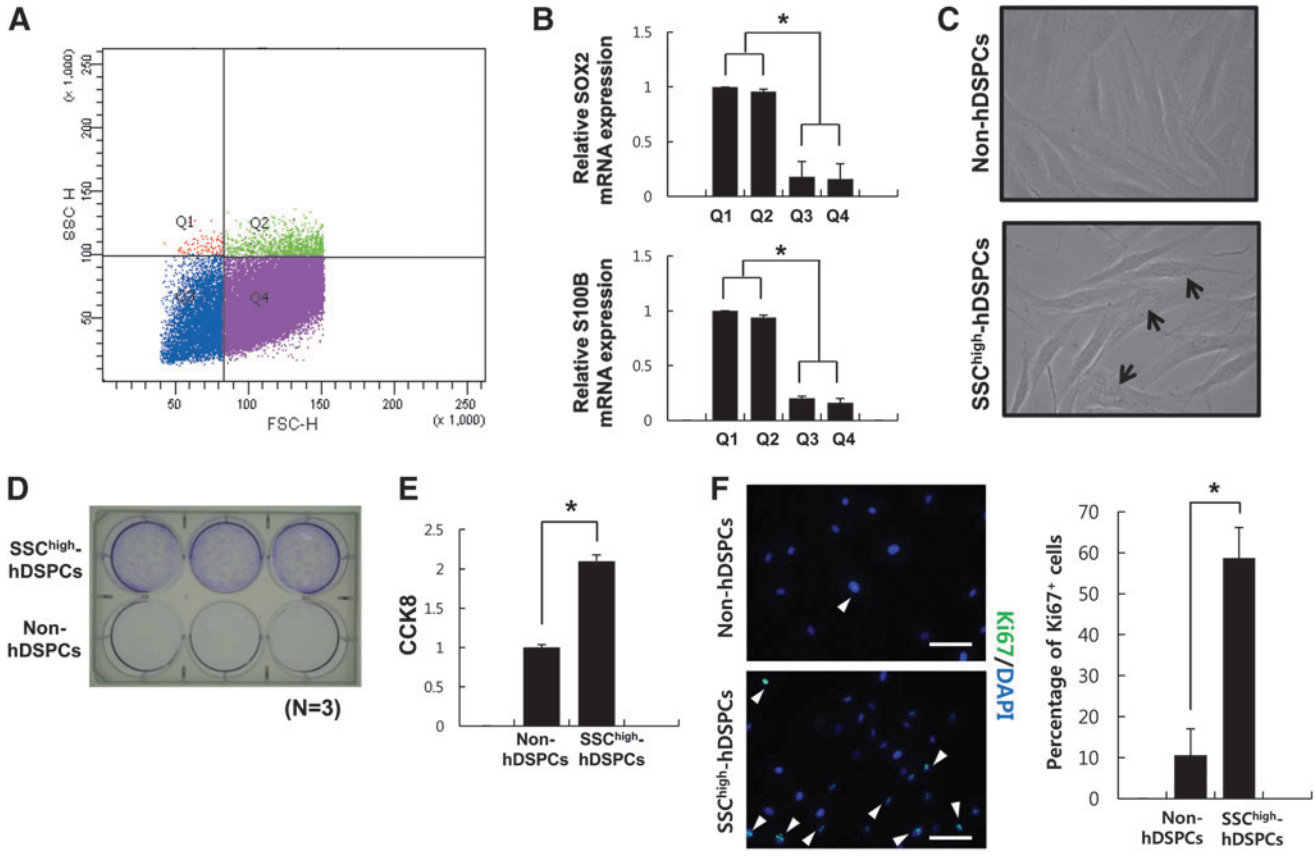

FIG. 2. Characterization of isolated SSC^{high}-hDSPCs. **(A)** Flow cytometry analysis of FSC/SSC in NHDFs. Cells were divided into 4 groups (Q1: FSC^{low}SSC^{high}; Q2: FSC^{high}SSC^{high}; Q3: FSC^{low}SSC^{low}; Q4: FSC^{high}SSC^{low}). **(B)** Real-time RT-PCR analysis of the SKP markers, *SOX2* and *S100B*. **(C)** Phase-contrast images of SSC^{high}-hDSPCs (*lower panel*) and non-hDSPCs (*upper panel*) isolated by a fluorescence-activated cell sorter. *Arrows* denote intracellular granule. **(D)** Cells grown in the NHDF growth medium for 10 days were examined using the colony-forming assay. **(E)** SSC^{high}-hDSPCs were significantly more proliferative as compared with the non-hDSPCs by the cell counting kit-8 analysis. **(F)** Non-hDSPCs (*upper panel*) or SSC^{high}-hDSPCs (*lower panel*) were stained with Ki67 (*arrowheads*). Scale bar: 100 μm. The quantity of cells expressing Ki67 is expressed as a percentage of the total cells counted after staining with DAPI. The data represent the mean ± SD of independent experiments run in triplicate. *$P < 0.01$. RT-PCR, reverse transcription–polymerase chain reaction; SKPs, skin-derived progenitors; DAPI, 4′,6-diamidino-2-phenylindole dihydrochloride; SD, standard deviation.

the differentiated cells derived from the SSC^{high}-hDSPCs were stained with Oil Red O (36 ± 4.58, $n = 3$). Densitometric quantification of Oil-Red-O-stained cells showed that lipid accumulation was increased by 7.6-fold in the SSC^{high}-hDSPCs compared with non-hDSPCs ($P < 0.01$) (Fig. 3C). These SSC^{high}-hDSPC-derived cells were also positively stained for perilipin on lipid droplets (Fig. 3B). Adipogenic differentiation was further confirmed by real-time RT-PCR. *PPARγ*, adiponectin, leptin, and *FABP4*, which are expressed in mature adipocytes, were highly expressed in the SSC^{high}-hDSPCs after 2 weeks of differentiation compared with non-hDSPCs ($P < 0.01$) (Fig. 3D). Thus, SSC^{high}-hDSPCs have the ability to differentiate into the adipogenic lineage.

After 3 weeks of culture in an osteogenic medium, over 60% of the SSC^{high}-hDSPC-derived cells stained positive for ALP (61.67 ± 6.12, $n = 3$) (Fig. 4A). When non-hDSPCs were differentiated with an osteogenic medium, very few cells showed weak ALP staining (Fig. 4A). Osteoblast-like cells were observed by osteocalcin staining after osteogenic induction (Fig. 4B). The expression of both osteoglycin and osteocalcin significantly increased in the SSC^{high}-hDSPCs after osteogenic induction compared with non-hDSPCs ($P < 0.01$) (Fig. 4C), suggesting that SSC^{high}-hDSPCs have the ability to differentiate into osteoblast-like cells.

Chondrogenic differentiation was evaluated after 14 days of culture in a chondrogenic differentiation condition. Safranin-O staining was used to detect the expression of proteoglycans, the extracellular matrix molecules synthesized by chondrocytes. A high level of Safranin-O staining was observed in the differentiated SSC^{high}-hDSPCs, indicating that these cells can differentiate into chondrogenic cell types (Fig. 5A). About 60% of the differentiated cells derived from the SSC^{high}-hDSPCs were positive for SOX9 after 2 weeks under differentiation conditions (58.67 ± 7.23, $n = 3$) (Fig. 5B). Real-time RT-PCR analysis revealed increased mRNA expression levels of the chondrocyte gene markers *COL2A* and aggrecan in the SSC^{high}-hDSPC-derived cells compared with non-hDSPCs ($P < 0.01$) (Fig. 5C). These results indicate that SSC^{high}-hDSPCs have the potential to differentiate into chondrocytes.

For neural induction, SSC^{high}-hDSPCs were plated on culture dishes coated with laminin/poly-D-lysine. After neural differentiation, the SSC^{high}-hDSPC-derived cells showed

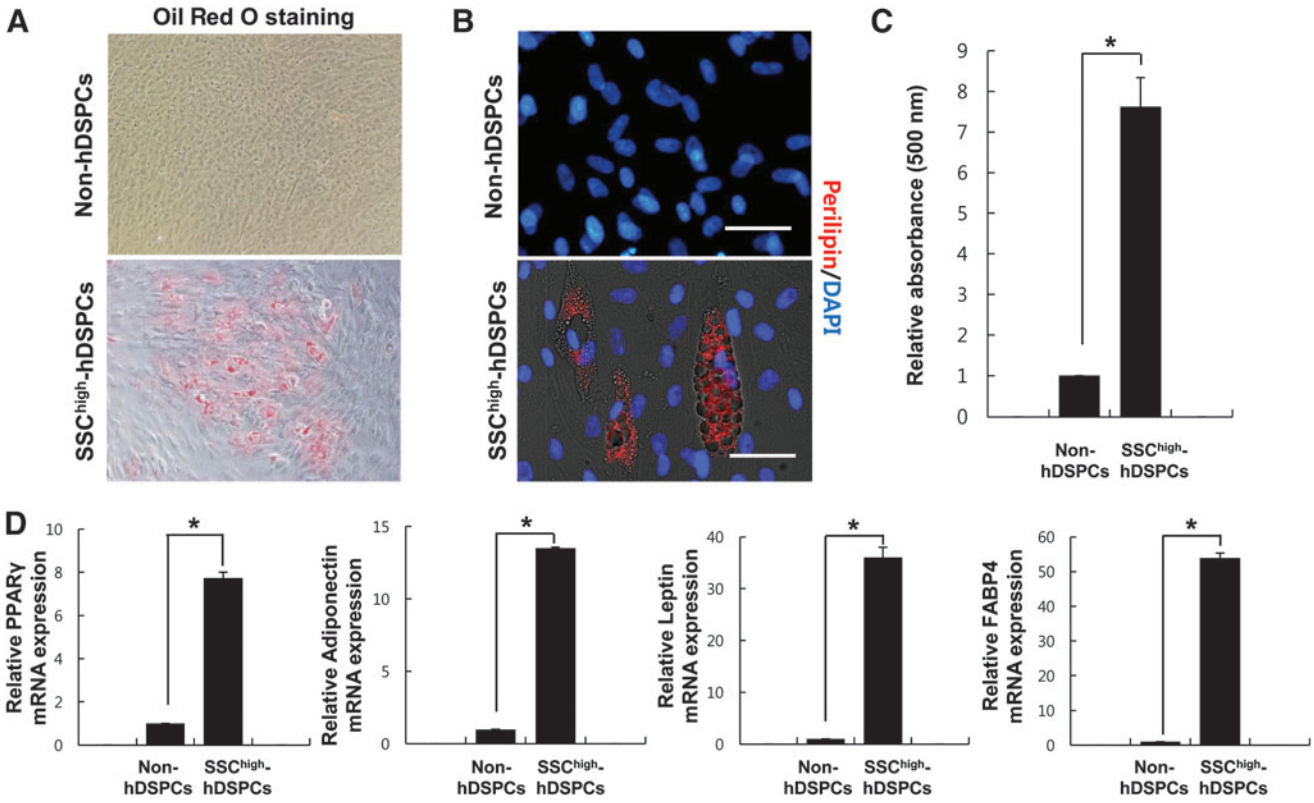

FIG. 3. Adipogenic differentiation of SSC^{high}-hDSPCs. Non-hDSPCs (*upper panel*) or SSC^{high}-hDSPCs (*lower panel*) were cultured in an adipogenic-inducing medium for 2 weeks (×400). **(A)** Oil-Red-O staining was positive in the differentiated SSC^{high}-hDSPCs. **(B)** Cells were stained for perilipin. Scale bar: 100 μm. **(C)** Oil-Red-O elution in differentiated cells. A significantly greater amount of Oil-Red-O was extracted from adipogenically differentiated SSC^{high}-hDSPCs than from non-hDSPCs. **(D)** Real-time RT-PCR analysis revealed upregulation of *PPARγ*, leptin, adiponectin, and *FABP4* mRNA expression upon adipogenic differentiation. Values represent means ± SD of independent experiments run in triplicate. *$P < 0.01$. PPARγ, peroxisome proliferator-activated receptor-gamma; FABP4, fatty acid-binding protein 4.

neural cell-like morphology. Expression of beta III tubulin (*Tuj1*) and MAP2 was detected in ~20%, and 10% of differentiated SSC^{high}-hDSPCs, respectively (20.66 ± 4.5, $n = 3$; 9.33 ± 2.3, $n = 3$), whereas no staining was detected in non-hDSPCs exposed to the same culture condition (Fig. 6A). Neural differentiation was further confirmed by real-time RT-PCR. The expression levels of both *MAP2* and nestin were significantly increased in the SSC^{high}-hDSPC-derived cells compared with non-hDSPCs ($P < 0.01$) (Fig. 6C).

Overall, these experiments demonstrated that SSC^{high}-hDSPCs have the in vitro potential to differentiate into not only mesodermal but also neuroectodermal cell types.

Discussion

It has long been believed that adult stem cells, which are present in most mammalian tissues, are necessary for maintaining normal tissue homeostasis, and are helpful for tissue repair and regeneration in response to various damages such as ultraviolet and oxidative stress [39–42]. Adult stem/progenitor cells are also known to exist in the dermis [13–20]. These cells can be characterized into various cell types, including those that differentiate into adipocytes, chondrocytes, smooth muscle cells, and osteoblasts, and those that differentiate into nonmesodermal cells, including neural cells, hepatocytes, and pancreatic cells [13–20,43,44].

The development of specific methods to easily isolate these adult stem cells from their host tissues is important not only to elucidate their molecular mechanisms, but also to investigate their physiological functions. According to previous reports, adult human dermal fibroblasts are a heterogeneous cell population comprising multipotent stem/progenitor cells and fully differentiated fibroblasts [16,28,45].

In our previous study, we found that putative hDSPCs can be enriched from NHDFs on the basis of their ability to adhere to collagen type IV, which is a binding partner of CD29, within 5 min [28]. These collagen type IV-sorted hDSPCs showed stem cell-like characteristics. That is, these collagen type IV-sorted hDSPCs exhibited a higher in vitro proliferative potential than non-hDSPCs, and were able to differentiate into mesodermal lineage and neuroectodermal lineage cells.

By real-time RT-PCR analysis, we found that there was no significant expression level of CD29 between collagen type IV-sorted hDSPCs and collagen type IV-sorted non-hDSPCs. This result could be occurred, because previous reports showed that NHDFs express CD29 [16,43]. Interestingly, we also found that we could enrich hDSPCs by gelatin coating within 5 min (data not shown), implying that their ability to adhere to collagen type IV or gelatin rapidly may be based on unknown physical characteristics. We further sought to develop a better method to isolate/enrich hDSPCs from

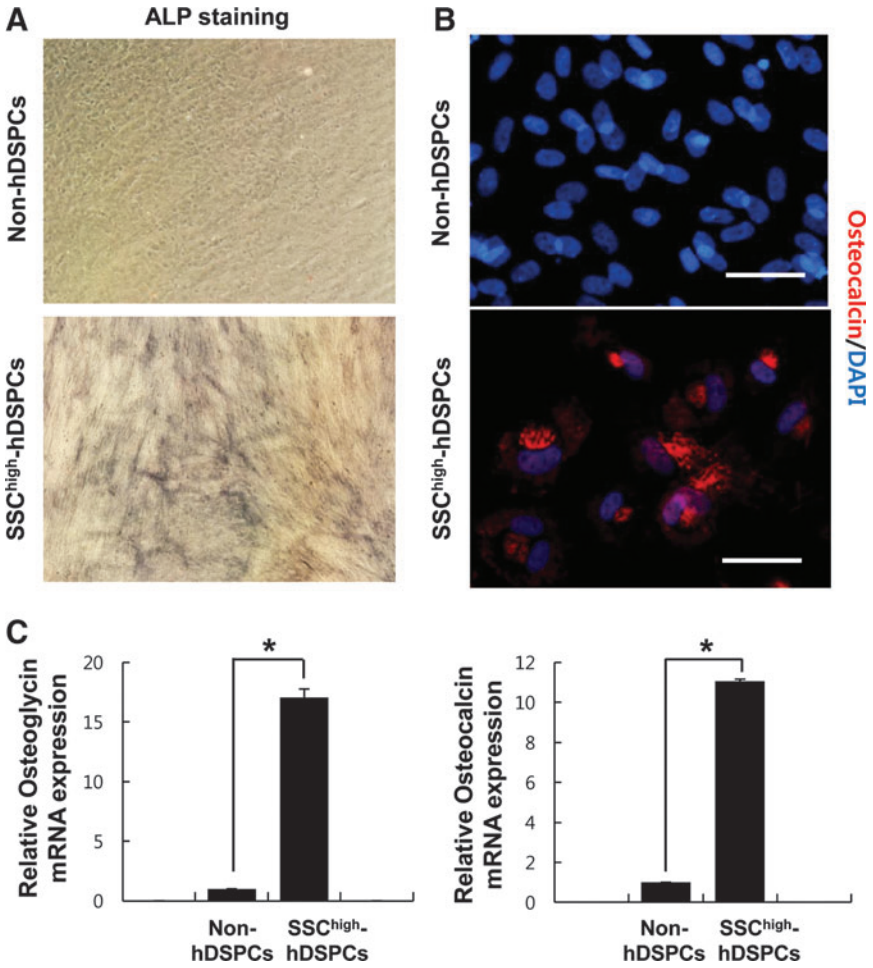

FIG. 4. Osteogenic differentiation of SSC^{high}-hDSPCs. Non-hDSPCs (*upper panel*) or SSC^{high}-hDSPCs (*lower panel*) were cultured in an osteogenic-inducing medium for 3 weeks (×400). **(A)** Alkaline phosphatase staining was positive in differentiated SSC^{high}-hDSPCs. **(B)** Positive immunostaining for osteocalcin was observed in the differentiated cells. Scale bar: 100 μm. **(C)** Real-time RT-PCR analysis revealed upregulation of osteoglycin and osteocalcin mRNA expression upon osteogenic differentiation. The data represent the mean ± SD of independent experiments run in triplicate. $^*P < 0.01$.

NHDFs using their other physical parameters, because collagen type IV-sorted hDSPCs are still heterogeneous. Several previous reports characterized neurosphere-derived cells or neurosphere-specific cells such as limbal cells by the FACS analysis and using several intracellular markers [46–48]. Thus, both granularity and size of collagen type IV-sorted hDSPCs were analyzed by flow cytometry. The percentage of cells in the SSC^{high} region was higher in collagen type IV-sorted hDSPCs than in collagen type IV-sorted non-hDSPCs by 3-fold, indicating the possibility that a subpopulation of NHDFs with higher granularity may be hDSPCs (Fig. 1). Therefore, we isolated SSC^{high}-hDSPCs using high-intracellular-granularity criteria (< 3.5% cells of total NHDFs). These SSC^{high}-hDSPCs showed a higher in vitro proliferative potential and higher expression levels of both *SOX2* and *S100B* than non-hDSPCs (Fig. 2B, D–F) and were multipotent and capable of differentiating into mesodermal as well as neuroectodermal lineages (Figs. 3–6). Interestingly, SOX9 was not detected in the nucleus when the SSC^{high}-hDSPCs were subjected to the chondrogenic differentiation condition. The cytoplasmic staining of SOX9 seemed to present a Golgi retention pattern, likely because of the immature state of the differentiating chondrocytes (Fig. 5B) [49].

Previous studies demonstrated that human dermis-derived multipotent fibroblasts by clonal isolation are negative for nestin and positive for vimentin representative intermediate filament proteins [16,45]. On the other hand, another group showed that SKPs derived from the human foreskin specifically express both nestin and vimentin in suspension cultures [13,15]. Interestingly, we demonstrated that SSC^{high}-hDSPCs showed no significant differences in the expression of nestin or vimentin compared with non-hDSPCs. Furthermore, we also found that there were no significant differences in the expression levels of other specific markers such as *SNAI2*, *TWIST1*, versican, and *CORIN* between the 2 cell populations (Supplementary Fig. S2). We previously reported that there were no meaningful differences in the expression levels of MSC-specific surface markers such as CD44, CD73, CD90, and CD105 between collagen type IV-sorted hDSPCs and collagen type IV-sorted non-hDSPCs [28]. Taken together, these results indicate that SSC^{high}-hDSPCs may be another type of progenitor cells derived from human dermis, which are different from the previously isolated multipotent fibroblasts and SKPs [13–16,45].

In our previous study [28], the relative percentage of collagen IV-sorted hDSPCs in NHDFs gradually decreased as passages increased. After 5 passages, even a small percentage of cells adhered to the collagen type-IV-coated culture dishes within 5 min showed no in vitro proliferative potential and multipotential differentiation capabilities. This phenomenon may be explained by some previous reports [50,51]. Liu et al. demonstrated that after dissociation from their physiological environment, SKPs rapidly undergo senescence and lose their self-renewal property, which is

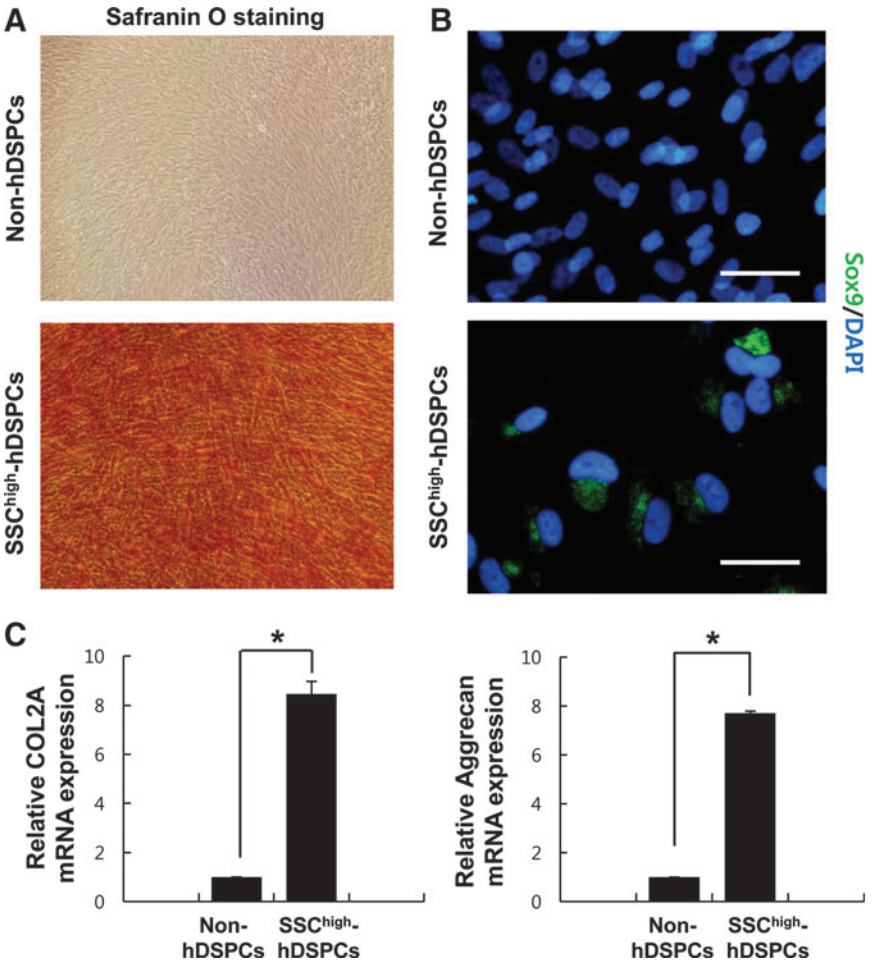

FIG. 5. Chondrogenic differentiation of SSC^{high}-hDSPCs. Non-hDSPCs (*upper panel*) or SSC^{high}-hDSPCs (*lower panel*) were cultured in a chondrogenic-inducing medium for 2 weeks (×400). **(A)** Safranin-O staining was positive in differentiated SSC^{high}-hDSPCs. **(B)** A SOX9 antibody was used to estimate chondrogenic differentiation. Scale bar: 100 μm. **(C)** Real-time RT-PCR analysis revealed upregulation of *COL2A* and aggrecan mRNA expression upon chondrogenic differentiation. The data represent the mean ± SD of independent experiments run in triplicate. *$P < 0.01$. *COL2A*, collagen type 2-alpha.

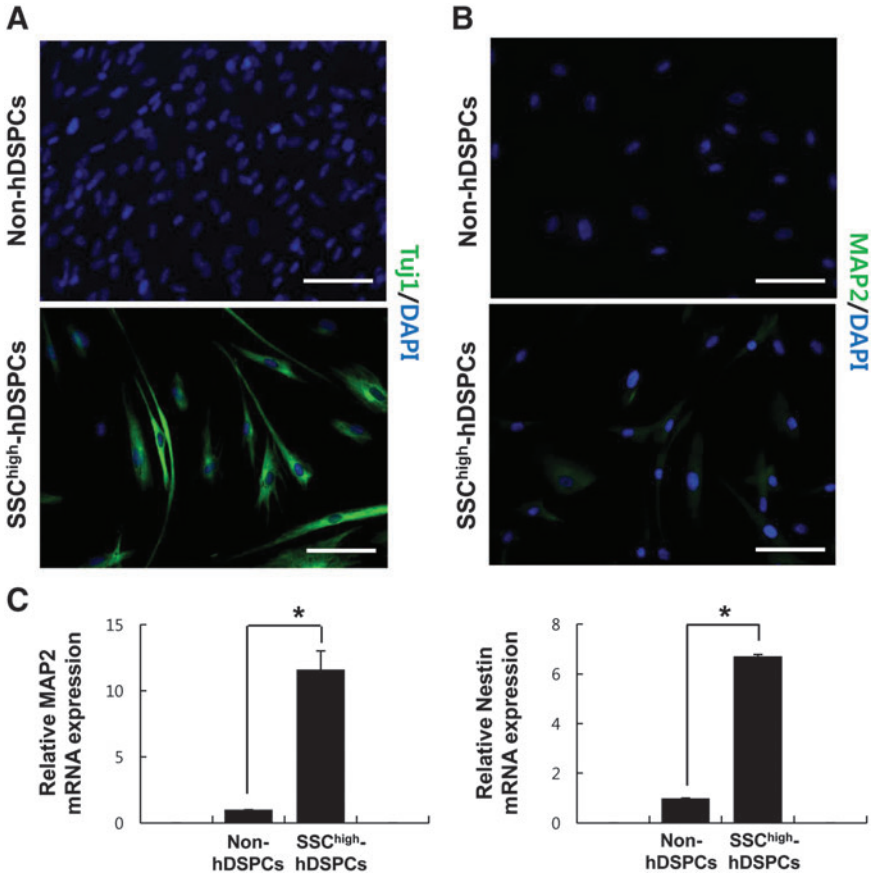

FIG. 6. Neurogenic differentiation of SSC^{high}-hDSPCs. Non-hDSPCs (*upper panel*) or SSC^{high}-hDSPCs (*lower panel*) were cultured in a neurogenic inducing medium for 10 days. **(A, B)** Immunostaining for beta-III tubulin (Tuj1) or MAP2 was positive in differentiated SSC^{high}-hDSPCs. Scale bar: 100 μm. **(C)** Real-time RT-PCR analysis revealed upregulation of *MAP2* and nestin mRNA expression upon neurogenic differentiation. The data represent the mean ± SD of independent experiments run in triplicate. *$P < 0.01$. *MAP2*, microtubule-associated protein 2.

mainly due to loss of Akt activity [50]. Another report suggested that TAp63 plays an important role in maintaining adult skin stem cells by modulating cellular senescence [51]. Thus, further studies are needed to elucidate the cellular mechanisms underlying senescence of hDSPCs under an in vitro environment.

According to previous reports [13,15,38], SKPs derived from adult human dermis can be expanded for extended periods of time under a specific medium. On the other hand, Gago et al. insisted that abundance and differentiation potential of human SKPs significantly decrease with the age in the medium supplemented with FBS under the attachment condition, providing conflicting results on the expansion of human SKPs [52]. Thus, we first examined whether stem-cell-like properties of SSC^{high}-hDSPCs are well maintained in the 10% FBS-DMEM under attachment condition or floating condition, which contributes to form a sphere. Real-time RT-PCR analysis revealed that expression levels of both *SOX2* and *S100B* in SSC^{high}-hDSPCs were significantly enhanced under the floating condition compared with the attachment condition (Supplementary Fig. S3A). These data seem to be similar to several previous reports [53–55]. They suggested that various types of stem cells increase their ability to maintain them in the undifferentiated state under the sphere-forming condition compared with the monolayer condition.

We further investigated whether SSC^{high}-hDSPCs can be able to form floating spheres in the SKP medium, which contains FGF2 and EGF, as described previously [13,15,38]. We found that SSC^{high}-hDSPCs exhibited higher expression levels of both *SOX2* and *S100B* under the SKP medium than under the 10% FBS-DMEM (Supplementary Fig. S3B). These results suggest that stem cell characteristics of SSC^{high}-hDSPCs can be relatively well maintained in the SKP medium under the floating condition, implying that these cells show similarity with human SKPs under this specific condition.

A cell population that can differentiate into adipogenic and osteogenic lineages has been isolated from hair follicles [56,57]. Therefore, we cannot rule out the possibility that SSC^{high}-hDSPCs may be derived from hair follicles, which are present in the dermis of breast and abdomen as well as scalp. Thus, we examined whether we can isolate SSC^{high}-hDSPCs using our current sorting criteria from NHDFs derived from neonatal foreskin, which does not have hair follicles. We could isolate SSC^{high}-hDSPCs from NHDFs derived from neonatal foreskin as well as NHDFs derived from breast and abdomen skin, indicating that the SSC^{high}-hDSPCs are not originated from only hair follicles. Real-time RT-PCR analysis also revealed that there were significant differences in the expression of specific markers such as *SOX2* and *S100B* in SSC^{high}-hDSPCs compared with non-hDSPCs, regardless of age, race, and gender (Supplementary Fig. S4). In addition, we found that there were no differences in dermal papilla markers such as *CORIN* and versican among samples (Supplementary Fig. S4).

In the present study, we isolated SSC^{high}-hDSPCs using the characteristics of high intracellular granularity by flow cytometry, indicating that NHDFs do not exist as uniform characteristics. Such morphological differences could serve as a useful indicator for identifying cellular characteristics that induce cellular growth, arrest, or death. There are a few literatures concerning the meaning of the intracellular granularity in specific cell types [46–48]. Bez et al. [46] investigated whether neurosphere-derived cells with physical properties such as FSC/SSC parameters can be identified in each G0/G1, S, and G2/M phases of the cell cycle. They observed that no significant fluctuations in the percentage of cells are present in different phases of the cell cycle [46]. Another previous report showed that limbal cells have lower cytosol granularity than the corneal cells by using the parameter of SSC, which can be applicable for discriminating specific cells among various cells [47]. Murayama et al. reported that adult-specific neural stem cells in FSC/SSC profiles of the developing stratum gain more cellular granularity between E14.5 and P1-3 [48]. At present, we used the high intracellular granularity as a parameter for enrichment of hDSPCs, but its biological meaning needs to be elucidated.

The current method for isolating SSC^{high}-hDSPCs is better than our previous collagen IV-sorting method [28] in the aspect of cell homogeneity, which is deduced from the results of biochemical and morphological comparison of 2 cell populations (Supplementary Fig. S5). However, this present approach still has a limitation that a subset of SSC^{high}-hDSPCs may include some non-hDSPCs. Homogenous hDSPCs can be isolated by identification of specific surface markers, which will also provide an efficient way for studying the physiological roles of hDSPCs. Although specific cell surface markers of multipotent fibroblasts or SKPs have been extensively explored [15,16,45,58,59], no unique markers have been definitively established. Thus, we will investigate novel specific markers for the isolation of the homogenous hDSPCs populations. We will carry out various trials such as a microarray analysis and other screening methods for surface markers on SSC^{high}-hDSPCs to identify specific cell surface markers, which may be useful for isolating hDSPCs with high purity.

In summary, we have shown that hDSPCs can be efficiently enriched by FACS using a structural property, intracellular granularity, as a sorting parameter. We found that these SSC^{high}-hDSPCs exhibited stemness properties, which may contribute to enhance wound repair and recover skin homeostasis in aged human skin.

Acknowledgments

This study was partly supported by a grant of the Korea Healthcare Technology R&D Project Ministry of Health & Welfare, Republic of Korea (grant no.: A103017).

Author Disclosure Statement

The authors state no conflict of interest.

References

1. Young HE, C Duplaa, R Katz, T Thompson, KC Hawkins, AN Boev, NL Henson, M Heaton, R Sood, et al. (2005). Adult-derived stem cells and their potential for use in tissue repair and molecular medicine. J Cell Mol Med 9:753–769.
2. Pereira RF, KW Halford, MD O'Hara, DB Leeper, BP Sokolov, MD Pollard, O Bagasra and DJ Prockop. (1995).

Cultured adherent cells from marrow can serve as long-lasting precursor cells for bone, cartilage, and lung in irradiated mice. Proc Natl Acad Sci U S A 92:4857–4861.
3. Pittenger MF, AM Mackay, SC Beck, RK Jaiswal, R Douglas, JD Mosca, MA Moorman, DW Simonetti, S Craig and DR Marshak. (1999). Multilineage potential of human mesenchymal stem cells. Science 284:143–147.
4. Anderson DJ, FH Gage and IL Weissman. (2001). Can stem cells cross lineage boundaries? Nat Med 7:393–395.
5. Jiang Y, BN Jahagirdar, RL Reinhardt, RE Schwartz, CD Keene, XR Ortiz-Gonzalez, M Reyes, T Lenvik, et al. (2002). Pluripotency of mesenchymal stem cells derived from adult marrow. Nature 418:41–49.
6. Jiang Y, B Vaessen, T Lenvik, M Blackstad, M Reyes and CM Verfaillie. (2002). Multipotent progenitor cells can be isolated from postnatal murine bone marrow, muscle, and brain. Exp Hematol 30:896–904.
7. Zuk PA, M Zhu, H Mizuno, J Huag, JW Futrell, AJ Katz, P Benhaim, HP Lorenz and MH Hedrick. (2001). Multilineage cells from human adipose tissue: implications for cell-based therapies. Tissue Eng 7:211–218.
8. Zuk PA, M Zhu, P Ashjian, DA De Ugarte, JI Huang, H Mizuno, ZC Alfonso, JK Fraser, P Benhaim and MH Hedrick. (2002). Human adipose tissue is a source of multipotent stem cells. Mol Biol Cell 13:4279–4295.
9. Lee MW, MS Yang, JS Park, HC Kim, YJ Kim and J Choi. (2005). Isolation of mesenchymal stem cells from cryopreserved human umbilical cord blood. Int J Hematol 81: 126–130.
10. Fukuchi Y, H Nakajima, D Sugiyama, I Hirose, T Kitamura and K Tsuji. (2004). Human placenta-derived cells have mesenchymal stem/progenitor cell potential. Stem Cells 22:649–658.
11. Blanpain C and E Fuchs. (2006). Epidermal stem cells of the skin. Annu Rev Cell Dev Biol 22:339–373.
12. Fuchs E. (2009). Finding one's niche in the skin. Cell Stem Cell 4:499–502.
13. Toma JG, M Akhavan, KJ Fernandes, F Barnabé-Heider, A Sadikot, DR Kaplan and FD Miller. (2001). Isolation of multipotent adult stem cells from the dermis of mammalian skin. Nat Cell Biol 3:778–784.
14. Fernandes KJ, IA McKenzie, P Mill, KM Smith, M Akhavan, F Barnabé-Heider, J Biernaskie, A Junek, NR Kobayashi, et al. (2004). A dermal niche for multipotent adult skin-derived precursor cells. Nat Cell Biol 6:1082–1093.
15. Toma JG, IA McKenzie, D Bagli and FD Miller. (2005). Isolation and characterization of multipotent skin-derived precursors from human skin. Stem Cells 23:727–737.
16. Chen FG, WJ Zhang, D Bi, W Liu, X Wei, FF Chen, L Zhu, L Cui and Y Cao. (2007). Clonal analysis of nestin(−) vimentin(+) multipotent fibroblasts isolated from human dermis. J Cell Sci 120:2875–2883.
17. Deng Y, JC Hu and KA Athanasiou. (2007). Isolation and chondroinduction of a dermis isolated, aggrecan-sensitive subpopulation with high chondrogenic potential. Arthritis Rheum 56:168–176.
18. Biernaskie J, M Paris, O Morozova, BM Fagan, M Marra, L Pevny and FD Miller. (2009). SKPs derive from hair follicle precursors and exhibit properties of adult dermal stem cells. Cell Stem Cell 5:610–623.
19. Driskell RR, A Giangreco, KB Jensen, KW Mulder and FM Watt. (2009). Sox2-positive dermal papilla cells specify hair follicle type in mammalian epidermis. Development 7136: 2815–2823.
20. Junker JP, P Sommar, M Skog, H Johnson and G Kratz. (2010). Adipogenic, chondrogenic and osteogenic differentiation of clonally derived human dermal fibroblasts. Cells Tissues Organs 191:105–118.
21. Amoh Y, L Li, R Campillo, K Kawahara, K Katsuoka, S Penman and RM Hoffman. (2005). Implanted hair follicle stem cells form Schwann cells that support repair of severed peripheral nerves. Proc Natl Acad Sci U S A 102:17734–17738.
22. Ohyama M, A Terunuma, CL Tock, MF Radonovich, CA Pise-Masison, SB Hopping, JN Brady, MC Udey and JC Vogel. (2006). Characterization and isolation of stem cell-enriched human hair follicle bulge cells. J Clin Invest 116:249–260.
23. Rendl M, L Lewis and E Fuchs. (2005). Molecular dissection of mesenchymal-epithelial interactions in the hair follicle. PLoS Biol 3:e331.
24. Wegner M and CC Stolt. (2005). From stem cells to neurons and glia: a Soxist's view of neural development. Trends Neurosci 28:583–588.
25. Takahashi K and S Yamanaka. (2006). Induction of pluripotent stem cells from mouse embryonic and adult fibroblast cultures by defined factors. Cell 126:663–676.
26. Takahashi K, K Tanabe, M Ohnuki, M Narita, T Ichisaka, K Tomoda and S Yamanaka. (2007). Induction of pluripotent stem cells from adult human fibroblasts by defined factors. Cell 131:861–872.
27. Park SB, KW Seo, AY So, MS Seo, KR Yu, SK Kang and KS Kang. (2011). SOX2 has a crucial role in the lineage determination and proliferation of mesenchymal stem cells through Dickkopf-1 and c-MYC. Cell Death Differ 19:534–545.
28. Shim JH, HH Kang, TR Lee and DW Shin. (2012). Enrichment and characterization of human dermal stem/progenitor cells using collagen, Type IV. J Dermatol Sci 67:202–205.
29. Scott MA, VT Nguyen, B Levi and AW James. (2011). Current methods of adipogenic differentiation of mesenchymal stem cells. Stem Cells Dev 10:1793–1804.
30. Montemurro T, G Andriolo, E Montelatici, G Weissmann, M Crisan, MR Colnaghi, P Rebulla, F Mosca, B Péault and L Lazzari. (2011). Differentiation and migration properties of human foetal umbilical cord perivascular cells: potential for lung repair. J Cell Mol Med 15:796–808.
31. Gao L, R McBeath and CS Chen. (2010). Stem cell shape regulates a chondrogenic versus myogenic fate through Rac1 and N-cadherin. Stem Cells 28:564–572.
32. D'Ippolito G, S Diabira, GA Howard, P Menei, BA Roos and PC Schiller. (2004). Marrow-isolated adult multilineage inducible (MIAMI) cells, a unique population of postnatal young and old human cells with extensive expansion and differentiation potential. J Cell Sci 117:2971–2981.
33. Alexander CM, J Puchalski, KS Klos, N Badders, L Ailles, CF Kim, P Dirks and MJ Smalley. (2009). Separating stem cells by flow cytometry: reducing variability for solid tissues. Cell Stem Cell 5:579–583.
34. Hughes OR, R Stewart, I Dimmick and EA Jones. (2009). A critical appraisal of factors affecting the accuracy of results obtained when using flow cytometry in stem cell investigations: where do you put your gates? Cytometry A 75: 803–810.
35. Pochampally R. (2008). Colony forming unit assays for MSCs. Methods Mol Biol 449:83–91.
36. Morris RJ, Y Liu, L Marles, Z Yang, C Trempus, S Li, JS Lin, JA Sawicki and G Cotsarelis. (2004). Capturing and profiling adult hair follicle stem cells. Nat Biotechnol 22:411–417.

37. Sekiya I, BL Larson, JR Smith, R Pochampally, JG Cui and DJ Prockop. (2002). Expansion of human adult stem cells from bone marrow stroma: conditions that maximize the yields of early progenitors and evaluate their quality. Stem Cells 20:530–541.
38. Joannides A, P Gaughwin, C Schwiening, H Majed, J Sterling, A Compston and S Chandran. (2004). Efficient generation of neural precursors from adult human skin: astrocytes promote neurogenesis from skin-derived stem cells. Lancet 364:172–178.
39. Prockop DJ. (1997). Marrow stromal cells as stem cells for nonhematopoietic tissues. Science 276:71–77.
40. Weissman IL. (2000). Stem cells: units of development, units of regeneration, and units in evolution. Cell 100:157–168.
41. Mezey E, S Key, G Vogelsang, I Szalayova, GD Lange and B Crain. (2003). Transplanted bone marrow generates new neurons in human brains. Proc Natl Acad Sci U S A 100: 1364–1369.
42. Li L and H Clevers. (2010). Coexistence of quiescent and active adult stem cells in mammals. Science 327:542–545.
43. Lysy PA, F Smets, C Sibille, M Najimi and EM Sokal. (2007). Human skin fibroblasts: from mesodermal to hepatocyte-like differentiation. Hepatology 46:1574–1585.
44. Bi D, FG Chen, WJ Zhang, GD Zhou, L Cui, W Liu and Y Cao. (2010) Differentiation of human multipotent dermal fibroblasts into islet-like cell clusters. BMC Cell Biol 11:46.
45. Manini I, L Gulino, B Gava, E Pierantozzi, C Curina, D Rossi, A Brafa, C D'Aniello and V Sorrentino. (2011). Multipotent progenitors in freshly isolated and cultured human mesenchymal stem cells: a comparison between adipose and dermal tissue. Cell Tissue Res 344:85–95.
46. Bez A, E Corsini, D Curti, M Biggiogera, A Colombo, RF Nicosia, SF Pagano and EA Parati.(2003). Neurosphere and neurosphere-forming cells: morphological and ultrastructural characterization. Brain Res 993:18–29.
47. Romano AC, EM Espana, SH Yoo, MT Budak, JM Wolosin and SC Tseng. (2003). Different cell sizes in human limbal and central corneal basal epithelia measured by confocal microscopy and flow cytometry. Invest Ophthalmol Vis Sci 44:5125–5129.
48. Murayama A, Y Matsuzaki, A Kawaguchi, T Shimazaki and H Okano. (2002). Flow cytometric analysis of neural stem cells in the developing and adult mouse brain. J Neurosci Res 69:837–847.
49. Fauquier T, K Rizzoti, M Dattani, R Lovell-Badge and IC Robinson. (2008). SOX2-expressing progenitor cells generate all of the major cell types in the adult mouse pituitary gland. Proc Natl Acad Sci U S A 105:2907–2912.
50. Liu S, S Liu, X Wang, J Zhou, Y Cao, F Wang and E Duan. (2011). The PI3K-Akt pathway inhibits senescence and promotes self-renewal of human skin-derived precursors *in vitro*. Aging Cell 10:661–674.
51. Su X, M Paris, YJ Gi, KY Tsai, MS Cho, YL Lin, JA Biernaskie, S Sinha, C Prives, et al. (2009). TAp63 prevents premature aging by promoting adult stem cell maintenance. Cell Stem Cell 5:64–75.
52. Gago N, V Pérez-López, JP Sanz-Jaka, P Cormenzana, I Eizaguirre, A Bernad and A Izeta. (2009). Age-dependent depletion of human skin-derived progenitor cells. Stem Cells 27:1164–1172.
53. Shimizu R, K Okabe, Y Kubota, A Nakamura-Ishizu, H Nakajima and K Kishi. (2011). Sphere formation restores and confers hair-inducing capacity in cultured mesenchymal cells. Exp Dermatol 20:679–681.
54. Ylöstalo JH, TJ Bartosh, K Coble and DJ Prockop. (2012). Human mesenchymal stem/stromal cells cultured as spheroids are self-activated to produce prostaglandin E2 that directs stimulated macrophages into an anti-inflammatory phenotype. Stem Cells 30:2283–2296.
55. Yu KR, SR Yang, JW Jung, H Kim, K Ko, DW Han, SB Park, SW Choi, SK Kang, H Schöler and KS Kang. (2012). CD49f enhances multipotency and maintains stemness through the direct regulation of OCT4 and SOX2. Stem Cells 30:876–887.
56. Riekstina U, R Muceniece, I Cakstina, I Muiznieks and J Ancans. (2008). Characterization of human skin-derived mesenchymal stem cell proliferation rate in different growth conditions. Cytotechnology 58:153–162.
57. Riekstina U, I Cakstina, V Parfejevs, M Hoogduijn, G Jankovskis, I Muiznieks, R Muceniece and J Ancans. (2009). Embryonic stem cell marker expression pattern in human mesenchymal stem cells derived from bone marrow, adipose tissue, heart and dermis. Stem Cell Rev 5:378–386.
58. Jahoda CA, J Whitehouse, AJ Reynolds and N Hole. (2003). Hair follicle dermal cells differentiate into adipogenic and osteogenic lineages. Exp Dermatol 12:849–859.
59. Hoogduijn MJ, Gorjup E and Genever PG. (2006). Comparative characterization of hair follicle dermal stem cells and bone marrow mesenchymal stem cells. Stem Cells Dev 15:49–60.

Address correspondence to:
Dr. Dong Wook Shin
Bioscience Research Institute
Amorepacific Corporation R&D Center
314-1, Bora-dong, Giheung-gu
Yongin-si, Geyonggi-do 446-729
Republic of Korea

E-mail: biopang@amorepacific.com

Dr. Tae Ryong Lee
Bioscience Research Institute
Amorepacific Corporation R&D Center
314-1, Bora-dong, Giheung-gu
Yongin-si, Gyeonggi-do 446-729
Republic of Korea

E-mail: trlee@amorepacific.com

Received for publication May 8, 2012
Accepted after revision November 26, 2012
Prepublished on Liebert Instant Online January 22, 2013